



Free Flow at the Interface of Porous Surfaces: A Generalization of the Taylor Brush Configuration

U. SHAVIT^{1,*}, R. ROSENZWEIG¹ and S. ASSOULINE²

¹*Civil and Environment Engineering, Technion, Haifa 32000, Israel*

²*Institute of Soil, Water and Environmental Sciences, Volcani Center, A.R.O., Bet Dagan, 50250, Israel*

(Received: 10 November 2002; in final form: 20 March 2003)

Abstract. A solution to the problem of shallow laminar water flow above a porous surface is essential when modeling phenomena such as erosion, resuspension, and mass transfer between the porous media and the flow above it. Previous studies proposed theoretical, experimental, and numerical insight with no single general solution to the problem. Many studies have used the Brinkman equation, while others showed that it does not represent the actual interface flow conditions. In this paper we show that the interface macroscopic velocity can be accurately modeled by introducing a modification to the Brinkman equation. A moving average approach was proved to be successful when choosing the correct representative elementary volume and comparing the macroscopic solution with the average microscopic flow. As the size of the representative elementary volume was found to be equal to the product of the square root of the permeability and an exponential function of the porosity, a general solution is now available for any brush configuration. Given the properties of the porous media (porosity and permeability), the flow height and its driving force, a complete macroscopic solution of the interface flow is obtained.

Key words: Brinkman, Darcy, Stokes, REV, porous media, interface flow.

1. Introduction

Water flow above a porous media surface is an important but yet unsolved problem. It occurs in natural and man-made flows such as overland flow during rainfall events, some wetland flows, filtering, cooling, and is common in the electrical, chemical and food industry (e.g. heat sinks, solid catalyst beds). Modeling the interface flow velocity involves several inherent difficulties, which stem from the different nature of the fast moving flow above the interface and the slow porous media flow below the interface.

Comparing the flow inside the porous media with the flow in the non-porous region reveals some of these difficulties. The flow field above the interface is ill-defined as long as the velocity and shear are not specified at the interface. The flow inside the porous media is typically unknown since Darcy law fails to describe the penetration of the high velocities into the porous media. Momentum considerations

*Author for correspondence: e-mail: aguri@techunix.technion.ac.il

show that the Navier–Stokes equations, which are used to solve the flow above the interface, involve both inertial and viscous terms. These high order terms are missing in the Darcy law. Furthermore, the need to use a continuum formulation in the porous media leads to both macroscopic and microscopic considerations. Such a distinction does not necessarily exist in the flow outside the porous medium, away from the interface. Modeling the flow conditions in the vicinity of the interface requires, therefore, a technique that bridges the differences between these two distinct regions.

Two concepts were extensively used to solve the problem of flow over porous surfaces; the Brinkman equation (Brinkman, 1947) and Beavers and Joseph (1967) interface condition, both requiring empirical coefficients. The Brinkman equation, which is a viscous extension of the Darcy law, was proposed by Brinkman (1947) and developed later by Gray and O’Neill (1976), Whitaker (1999) and others. The empirical coefficients are the apparent viscosity, μ^* , and a variable permeability, k . The Beavers and Joseph interface condition relates the interface velocity gradient and the relative slip velocity through the permeability and an empirical slip coefficient, α_{BJ} .

The apparent viscosity, μ^* , is usually different from the fluid viscosity, μ , and represents the added resistance of the porous structure. It is expected, therefore, that the apparent viscosity will be larger than the fluid viscosity and will be dependant on the porous media properties (e.g. porosity and permeability). The literature, unfortunately, exhibits a remarkable disagreement with respect to the μ/μ^* ratio. Brinkman himself used an identical value for both viscosities. Howells (1974) and Happel and Brenner (1973) gave justification for using $\mu = \mu^*$ as a first approximation, while others proposed a wide verity of μ/μ^* ratios. The viscosity ratio in Koplik *et al.* (1983) and Nield and Bejan (1992) is $\mu/\mu^* > 1$, and in Adler and Mills (1979) and Kim and Russell (1985) is $\mu/\mu^* < 1$. Lundgren (1972) applied the Brinkman equation to solve the flow problem near a random bed of spheres. His solution shows that the apparent viscosity is larger than the fluid viscosity for high porosity and smaller for lower porosity.

The prescribed difficulties lead to a variety of formulations that include the Navier–Stokes equations, the Stokes equations, the Brinkman equation, the Forchheimer equation, and the Darcy law. Typically, the Navier–Stokes or Stokes equations are applied in the non-porous region and the Brinkman, Forchheimer or Darcy equations are applied inside the porous region. However, such a combination requires an exact specification of the interface location. Even when using one single equation for both domains, a step change in permeability or apparent viscosity requires an *a priori* knowledge of the interface location. It was shown that an exact interface location is often impossible to choose and that the solution of the velocity profile near the interface is sensitive to this unclear choice (Larson and Higdon, 1986). To avoid the need of a boundary condition at the interface, Basu and Khalili (1999) have developed a numerical solution using the ‘single domain approach’. However, they dropped out the Brinkman modification term in

the non-porous region and, therefore, did not avoid the need to define the interface location.

When solving the flow problem separately for either the porous or the non-porous regions, a boundary condition such as the Beavers and Joseph condition is needed,

$$\left. \frac{\partial \langle u \rangle}{\partial z} \right|_{z=0+} = \frac{\alpha_{BJ}}{\sqrt{k}} (\langle u \rangle|_{z=0+} - \langle u \rangle_d) \quad (1)$$

here $\langle u \rangle|_{z=0+}$ is the average interface velocity outside the porous media, $\langle u \rangle_d$ is the Darcian flux inside the porous media (far enough from the interface), and α_{BJ} is the Beavers and Joseph slip coefficient. The original analysis (Beavers and Joseph, 1967) was based on the velocity profile outside the porous media, where other authors examine the slip condition while solving both regions simultaneously. Where some studies have confirmed the Beavers and Joseph slip condition (Beavers *et al.*, 1970; Saffman, 1971; Zhou and Mendoza, 1993), others have shown that it varies as a function of flow conditions (e.g. Reynolds number, Couette versus Poiseuille, and the height of the up most boundary condition), microscopic structure, the fluid properties and the definition of the interface location (Richardson, 1971; Beavers *et al.*, 1974; Sahraoui and Kaviany, 1992).

Several studies have claimed that the available theories are not general enough and that small and large porosity media need to be treated separately (a diluteness assumption was needed in the Lundgren theory or when the Einstein correction was applied, Kaviany, 1995). Larson and Higdon (1986) presented numerical results of the micro-scale velocity field at the interface of a cylinders lattice. They found that the definition of the Beavers and Joseph slip coefficient is meaningful only for extremely dilute systems, and that the Brinkman equation succeeds to predict the flow above some geometries but fails in others.

The role of porosity is intuitively clear. As porosity increases, penetration, slip velocity and shear modification increase. James and Davis (2001) stated that the flow penetrates into the porous medium for porosity larger than 0.9 and that other cases are of little interest. This is not the case when solving a problem of shallow free flows (e.g. during a rainfall event). As the height of the water level, h , approaches zero, the magnitude of the Darcian velocity and the free boundary velocity becomes similar. The interface velocity is then important even when the porosity and permeability are low. A similar scenario may be developed in and around a preferential pathway through a porous medium (Jennings and Pisipati, 1999). A more general solution is therefore needed.

Recently, we have presented a solution to the velocity profile around the interface of a Cantor–Taylor brush (CTB) configuration (Shavit *et al.*, 2002), similar to configurations studied by Taylor (1971), Richardson (1971) and Vignes-Adler *et al.* (1987). The solution was based on an averaging procedure of the Navier–Stokes equations. Our analysis provides a set of three equations, which are used to predict the average velocity in the fluid phase, $\langle u \rangle^f$. This set of equations was named

the modified Brinkman equation (MBE). The comparison between the results of the average micro-scale Stokes equation and the MBE shows that optimizing the size of the representative elementary volume (REV) provides a good fit between the flow problem and the solution of the MBE. The velocity profile and its first derivative obtained by solving the MBE are continuous and reproduce the results of the average micro-scale Stokes equation. The analysis showed that the best fit is obtained when the height of the averaging representative volume, H_{rev} , is equal to 2.5 mm, regardless the water level and flow rate. No methodology was presented on how to choose the adequate value for H_{rev} . In the present paper we make a step forward by somehow generalize the MBE, apply it to laminar flows through a variety of groove geometries, analyze the effect of the porous media characterized by its porosity and permeability, and determine the functional relationships between H_{rev} and the porous media porosity and permeability.

2. Theory and Geometrical Configuration

The spatially averaged form of the unidirectional Navier–Stokes equation for a steady state fully developed flow, assuming a Newtonian fluid, a stagnant solid phase and constant liquid properties, as expressed in Shavit *et al.* (2002), is

$$-\frac{\partial \langle P \rangle}{\partial x} + \mu \left(\frac{\partial^2 \langle u \rangle}{\partial y^2} + \frac{\partial^2 \langle u \rangle}{\partial z^2} + \frac{1}{\forall} \int_S v_n \left(\frac{\partial u}{\partial y} \right) dS + \frac{1}{\forall} \int_S v_n \left(\frac{\partial u}{\partial z} \right) dS \right) = 0 \quad (2)$$

where u is the velocity component in the x -direction, y and z are the lateral and vertical coordinates, μ is the constant dynamic viscosity, P is the generalized pressure, \forall is the total volume of a representative elementary volume of the porous medium, S is the area of the interface between the two phases, and v_n is the unit normal vector along the interface pointing outwards from the liquid phase. The symbol $\langle \rangle$ represents an average over the total volume, and $\langle \rangle^f$ will represent an average over the volume fraction of the fluid phase ($\langle \rangle = \theta \langle \rangle^f$). Using a representative volume that covers the whole width of the CTB (in the y -direction) and a fixed width in the x -direction, substituting the fluid phase averaging using the porosity, $\langle u \rangle = \theta \langle u \rangle^f$, and replacing the integrals by a term like $\alpha \langle u \rangle^f$ (Gray and O’Neill, 1976; Whitaker, 1999), Equation (2) becomes

$$-\frac{\partial \langle P \rangle}{\partial x} + \mu \left(\frac{\partial^2 \theta \langle u \rangle^f}{\partial z^2} + \alpha \langle u \rangle^f \right) = 0 \quad (3)$$

where $\langle u \rangle$ represents the average of the velocity over the total volume, $\langle u \rangle^f$, the average of the velocity over the volume fraction of the liquid phase, θ , the water content, and α , the resistance coefficient (which is different than α_{BJ}). Equation (3) is similar to the Brinkman equation. Its second term is the Brinkman modification

to the Darcy law and its last term is the Brinkman modification to the Stokes equation.

The averaging procedure presented in Shavit *et al.* (2002) divides the flow domain into three regions within which the average porosity varies linearly from $\theta = 1$ outside the porous media to $\theta = n$ inside the porous media,

$$\theta = \begin{cases} 1, & z \geq \frac{H_{rev}}{2} \\ \left(\frac{1-n}{H_{rev}}\right)z + \left(\frac{1+n}{2}\right), & \frac{-H_{rev}}{2} \leq z \leq \frac{H_{rev}}{2} \\ n, & z \leq \frac{-H_{rev}}{2} \end{cases} \quad (4)$$

where n is the porosity of the porous media and z is the vertical coordinate with $z = 0$ at the interface. Consequently, Equation (3) becomes

$$\begin{cases} -\frac{\partial \langle P \rangle}{\partial x} + \mu \left(\frac{\partial^2 \langle u \rangle^f}{\partial z^2} \right) = 0, & z \geq \frac{H_{rev}}{2} \\ -\frac{\partial \langle P \rangle}{\partial x} + \mu \left(\left(\left(\frac{1-n}{H_{rev}} \right) z + \frac{1+n}{2} \right) \frac{\partial^2 \langle u \rangle^f}{\partial z^2} + \frac{-H_{rev}}{2} \leq z \leq \frac{H_{rev}}{2} \right. \\ \quad \left. + \frac{2(1-n)}{H_{rev}} \frac{\partial \langle u \rangle^f}{\partial z} - \alpha \langle u \rangle^f \right) = 0, \\ -\frac{\partial \langle P \rangle}{\partial x} + \mu \left(n \frac{\partial^2 \langle u \rangle^f}{\partial z^2} - \alpha \langle u \rangle^f \right) = 0, & z \leq \frac{-H_{rev}}{2} \end{cases} \quad (5)$$

Equation (5) is the generalized MBE. It is a simple differential equation, which assumes a linear change in porosity across the interface and contains three parameters; the porosity, n , the resistance coefficient, α , and the height of the representative averaging volume, H_{rev} . Where n and α are known for a given porous media, H_{rev} is to be specified. The MBE converges to the Brinkman equation in the porous region and to the Stokes equation in the non-porous region. The intermediate region reflects the transition between the Stokes flow and the porous media flow. As the velocity spatial variations in the porous region decay, the Brinkman equation and the Darcy equation become identical.

The applicability of the MBE (Eq. (5)) was investigated here using 37 geometrical sets representing a wide variety of brush configurations. Each set contains grooves and walls arranged symmetrically as detailed in Table I and illustrated in Figure 1. The sets were generated to create geometrical groups in which the porosity, n , varies while the resistance coefficient, α , is kept constant, and groups in which the resistance coefficient varies while keeping the porosity constant. Among these sets, set #23 (CTB studied by Shavit *et al.*, 2002), sets #9 and #33 are fractals. The depth of the grooves in all 37 sets was determined to assure a uniform vertical velocity profile in the center of the porous media. Table I lists the sequence of walls and grooves from the left end of the set to its symmetry line, providing the walls width p_i , the grooves width d_i , and the total width A . Note, that due to the symmetrical description, the actual width of the middle groove/wall is twice the value appearing in Table I. As an illustration, set #9 is shown in Figure 1. It consists of three grooves ($d_i = 2, 5$ and 2 mm) and four walls ($p_i = 4$ mm) with a

total width of 25 mm. The list of sets in Table I is sorted with an ascending order of the porosity, n , and the permeability, k .

The porosity of each set is defined as $n = \Sigma d_i/A$. The resistance coefficient, α , is computed as follows: deep inside the porous region, the Brinkman equation should become identical to the Darcy law. In that region, the second derivative of the velocity $\partial^2 \theta \langle u \rangle^f / \partial z^2$ vanishes, and Equation (5) is reduced to

$$-\frac{\partial \langle P \rangle}{\partial x} - \mu \alpha \langle u \rangle^f = 0, \quad \theta = n \quad (6)$$

Table I. Geometrical configuration of the investigated sets^a

Set #	p_1 (mm)	d_1 (mm)	p_2 (mm)	d_2 (mm)	p_3 (mm)	d_3 (mm)	A (mm)	n –	k (cm ²)	H_{rev} (mm)
1	8.5	1.5					20	0.15	0.001125	2.15
2	3	1	1				10	0.2	0.000167	0.7
3	4	1	4	1			20	0.2	0.000417	1.1
4	4	1					10	0.2	0.000667	1.4
5	4	0.5	4	1.5			20	0.2	0.001135	1.85
6	6	1.5					15	0.2	0.0015	2.1
7	8	2					20	0.2	0.002667	2.8
8	3.5	1.5					10	0.3	0.00225	1.9
9	4	2	4	2.5			25	0.36	0.0047	2.5
10	1	1.5	2	0.5			10	0.4	0.000646	0.8
11	1	1	2	1			10	0.4	0.000833	0.95
12	2	2	1				10	0.4	0.001333	1.2
13	1	0.5	2	1.5			10	0.4	0.002271	1.6
14	4	4	2				20	0.4	0.005333	2.35
15	1.9	1	1.9	1	1.9	2.3	20	0.43	0.004222	2.1
16	1	1.25	1	1.25	0.5		10	0.5	0.000651	0.7
17	1.25	1.5	1.25	1			10	0.5	0.001229	0.9
18	1	2	1.5	0.5			10	0.5	0.001417	1
19	2	2.5	0.5				10	0.5	0.002604	1.4
20	2.5	3	2.5	2			20	0.5	0.004917	1.9
21	1	0.5	1.5	2			10	0.5	0.005354	2
22	2.5	2.5					10	0.5	0.010417	2.8
23	2	2	2	3			18	0.556	0.01075	2.5
24	0.5	1.5	1	1.5	0.5		10	0.6	0.001125	0.7
25	0.5	1	1	2	0.5		10	0.6	0.0015	0.85
26	2	2	1				10	0.6	0.002	1
27	1	3	1				10	0.6	0.0045	1.5
28	1	1	1	2			10	0.6	0.0055	1.7
29	1	2	2	4	1		20	0.6	0.006	1.6

Table I. (continued)

Set #	p_1 (mm)	d_1 (mm)	p_2 (mm)	d_2 (mm)	p_3 (mm)	d_3 (mm)	A (mm)	n –	k (cm ²)	H_{rev} (mm)
30	4	4	2				20	0.6	0.008	1.9
31	1	0.5	1	2.5			10	0.6	0.010438	2.35
32	2	3					10	0.6	0.018002	3
33 ^b	1	1	1	1	1	5	25	0.64	0.008533	2
34	1	3	1.5	3.8	0.7		20	0.68	0.006823	1.4
35	0.4	2	0.4	2	0.2		10	0.8	0.002667	0.7
36	0.8	4	0.8	4	0.4		20	0.8	0.010667	1.3
37	0.5	3	0.5	3	0.75	2.25	20	0.825	0.008297	1.2

^a The width of the grooves and walls from the left end of the set to its symmetry line are represented by d_i and p_i , respectively. The actual width of the last groove or wall (at the symmetry line) is twice the value appearing in the table. A , n and k are the total width, the porosity and the permeability of the set, respectively. All dimensions are in mm. The last column shows the values of H_{rev} that provide the best fit between the results of Equations (5) and (10).

^b Set #33 contains two more walls and an extra groove: $p_4 = d_4 = 1$ mm and $p_5 = 0.5$ mm.

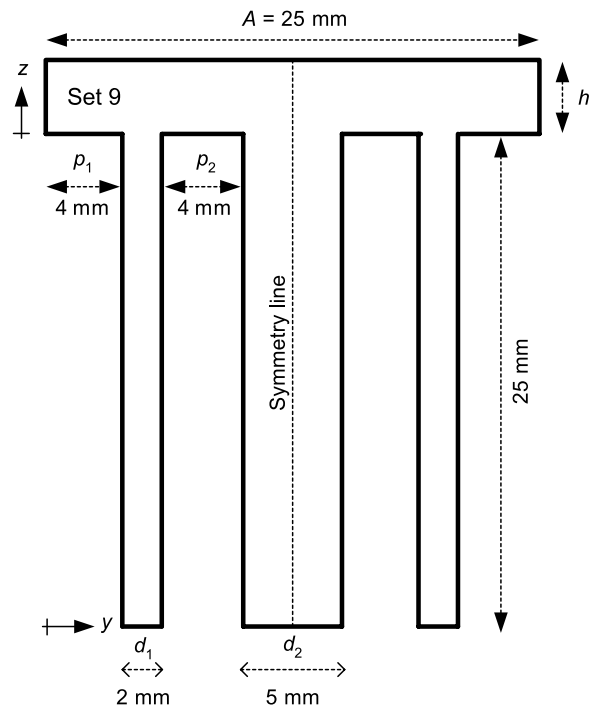


Figure 1. Geometrical configuration of set #9. z is the vertical coordinate with $z = 0$ at the interface, and h is the water height above the porous surface.

The volumetric flow rate of the fully developed laminar flow inside the grooves is

$$Q = -\frac{\partial \langle P \rangle}{\partial x} \frac{\sum d_i^3}{12\mu} \quad (7)$$

The permeability, $k = n/\alpha$, can now be calculated by combining Equations (6) and (7), applying the definition of the average velocity $\langle u \rangle^f = Q/An$, and computing α as follows

$$\alpha = 12 \frac{\sum d_i}{\sum d_i^3} \quad (8)$$

Table I lists the values of n and k of all the 37 sets. The density, viscosity and pressure gradient were specified for all the sets as $\rho = 1 \text{ g cm}^{-3}$, $\mu = 0.01 \text{ g cm}^{-1} \text{ s}^{-1}$, and $\partial \langle P \rangle / \partial x = -0.01 \text{ g cm}^{-2} \text{ s}^{-2}$, respectively.

3. Numerical Procedure

Numerical solutions were obtained using FEMLAB (Comsol), a finite element code developed for the MATLAB environment. The numerical solutions were accurate when validated against a variety of simple 1D and 2D flow problems (e.g. Poiseuille and Couette flows). The reported numerical solutions were generated by applying bilinear weight functions and as many triangle elements needed to obtain a stable and accurate solution. The 1D MBE and the 2D Stokes equation were solved using a maximum mesh size of 2304 elements and 35,056 elements, respectively, that cover one half of the symmetric domain.

4. Results and Discussion

The micro-scale velocity distribution inside the 37 sets was obtained by solving the 2D Stokes equation,

$$\frac{\partial^2 u}{\partial z^2} + \frac{\partial^2 u}{\partial y^2} = \frac{1}{\mu} \frac{dP}{dx} \quad (9)$$

applying a non-slip condition on the solid surfaces, a symmetry condition on the sides of the flow above the interface, and a zero shear condition at the top. A simulation of bounded flow was generated in three sets (#14, #20, and #35), applying a non-slip condition at the top. Solutions were examined for water heights of 2.5, 5, and 10 mm above the interface. The flow regime is laminar as shown by the range of Reynolds numbers (based on the height of the free flow region, h , and the highest velocity) extending between $Re = 1.47$ in set #9 ($h = 2.5 \text{ mm}$) and $Re = 57.9$ in set 36 ($h = 10 \text{ mm}$). The solutions shown in Figure 2 represent the micro-scale velocity distribution inside sets #9 and #33 (Table I) for a water height of $h = 2.5 \text{ mm}$. High velocities appear above the center of the wide grooves. These relatively high velocities influence both the macroscopic slip velocity and

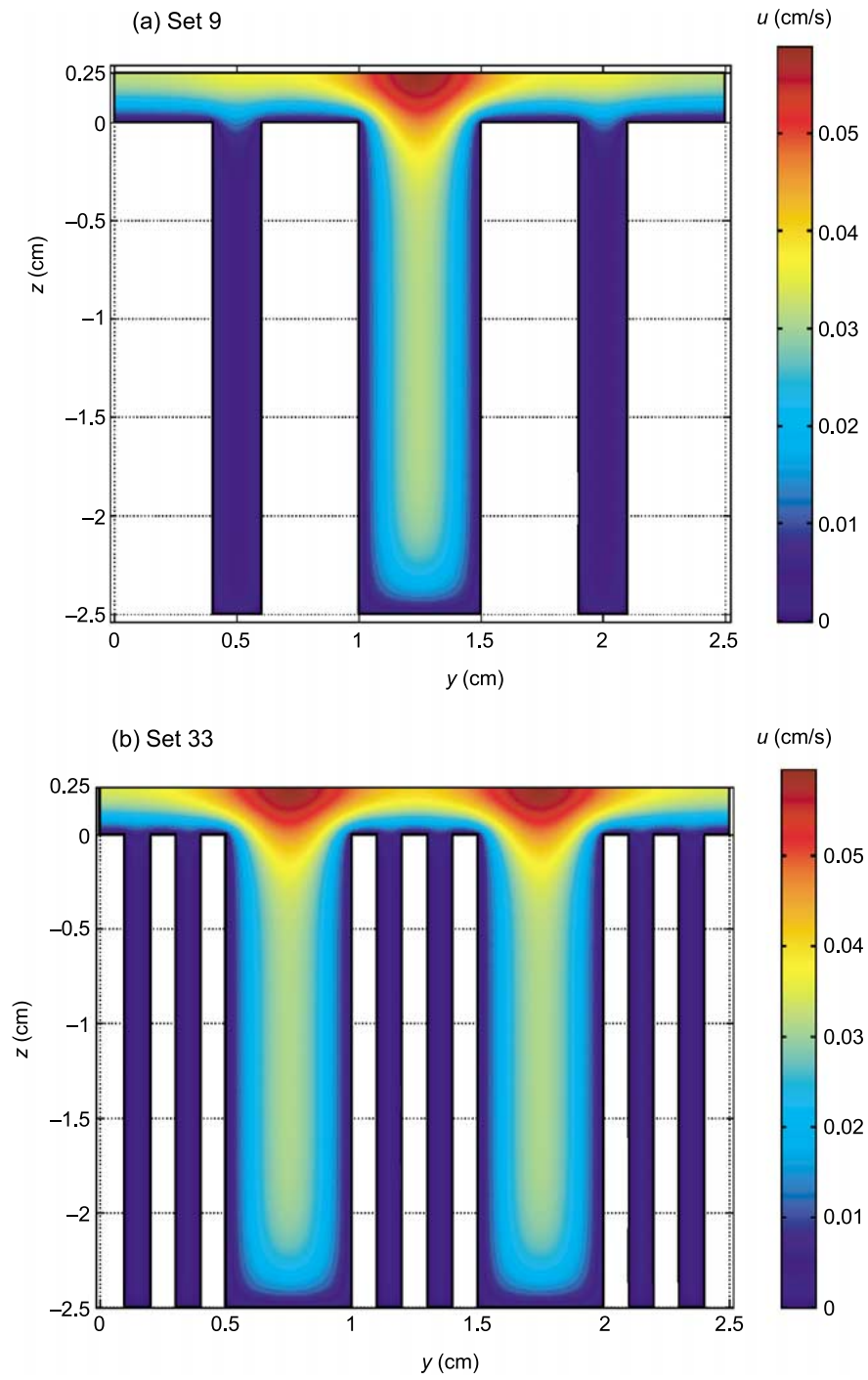


Figure 2. The micro-scale velocity distribution inside sets #9 and #33 obtained by solving the 2D Stokes equation for $h = 2.5$ mm.

the velocity gradient at the interface. As was shown in the case of set #23 (Shavit *et al.*, 2002), the velocity in the narrow grooves is small. The conclusion is that these narrow grooves do not significantly change the flow field, although they may play a significant role in transport processes.

It is assumed that the macro-scale description of the velocity is given by a moving average procedure applied on the micro-scale velocity distribution. The definition of this ‘real’ macro-scale description is given by

$$\langle u \rangle^f(z) = \frac{1}{AH_{\text{rev}}} \int_{AH_{\text{rev}}} u(y, z, z') dy dz' \quad (10)$$

where u represents the solution of Equation (9), and z' is an internal coordinate varying between $z - H_{\text{rev}}/2$ and $z + H_{\text{rev}}/2$ (Sahraoui and Kaviani, 1992). While the size of H_{rev} plays a major role in the MBE ability to describe the macro-scale velocity, the macroscopic velocity profile obtained by Equation (10) is less sensitive to the size of H_{rev} (Shavit *et al.*, 2002). The velocity profile obtained by the MBE (Eq. (5)) was compared with the results of Equation (10). The values of H_{rev} that provided the best fit between Equations (5) and (10) were identified and listed in Table I. The best fit between the solutions was generated by varying the value of H_{rev} , applying a step size of 0.1 mm and a careful examination of the slip velocity obtained by the two equations. A good fit was found for all 37 sets with some deviation at the lower end of the penetration region and near the lower boundary at the floor of the porous media. This last region of deviation is of secondary importance. Figure 3 shows a comparison between the solutions of the two equations for set #9. Similarly to our previous results (Shavit *et al.*, 2002), the two subplots demonstrate that the correct H_{rev} is general, regardless the water height ($h = 2.5, 10$ mm). The sudden change in the Stokes velocity curve at $z = -H_{\text{rev}}/2$ is due to the sudden change of porosity at $z = 0$. The smooth velocity curve generated by the MBE is a result of our volume average approach. While some studies applied an area averaging (e.g. Martys *et al.*, 1994), others have used a volume averaging (e.g. Basu and Khalili, 1999). Sahraoui and Kaviani (1992) have examined them both and even suggested a variable volume averaging technique. However, most of these studies have overlooked the problem of the size of the elementary volume used for the averaging process.

It is conceivable that H_{rev} is related to the porous media properties (n and k), and to their effect on the penetration depth. Since the penetration depth can be approximated by the square root of the permeability (*‘the Brinkman screening distance’*), the following relationship is suggested

$$H_{\text{rev}}(n, k) = f(n)\sqrt{k} \quad (11)$$

Based on the data in Table I, the function $f(n)$ is well approximated by an exponential function, as shown in Figure 4. Consequently, the functional relationship between H_{rev} and the porous media properties, n and k , is of the form

$$H_{\text{rev}}(n, k) = a e^{-bn} \sqrt{k} \quad (12)$$

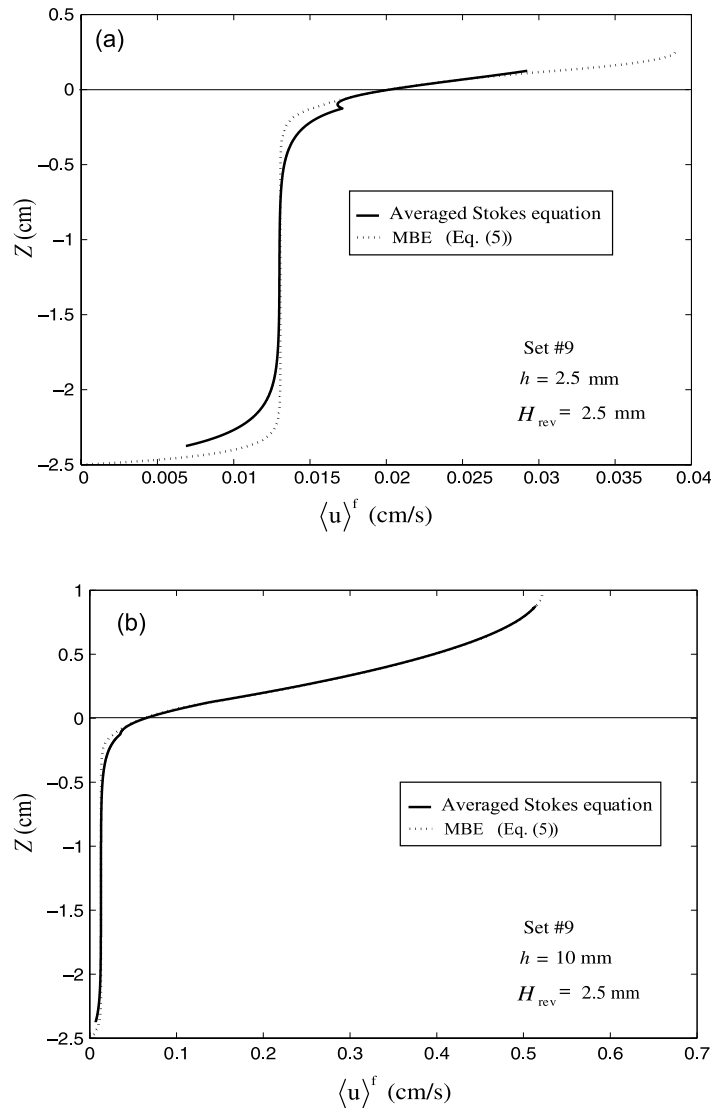


Figure 3. The velocity profile obtained by the 1D MBE (Eq. (5)) compared with the macro-scale description of the velocity (Eq. (10)) resulting from the solution of the 2D Stokes equation, for set #9 and two water heights ($h = 2.5$ and 10 mm).

with $a \cong 8.49$ and $b \cong 2.29$. The combination of the MBE (Eq. (5)) and Equation (12) provides now an accurate tool for calculating the vertical macroscopic velocity profile given the fundamental properties of the porous media, n and k , the fluid viscosity, the flow height and the flow driving force $\partial \langle P \rangle / \partial x$. This is a general solution that may be applied to any laminar flow problem that involves an interface between a porous media that consists of series of deep grooves and a relatively fast moving flow region. Moreover, we have tested the applicability of the MBE when a

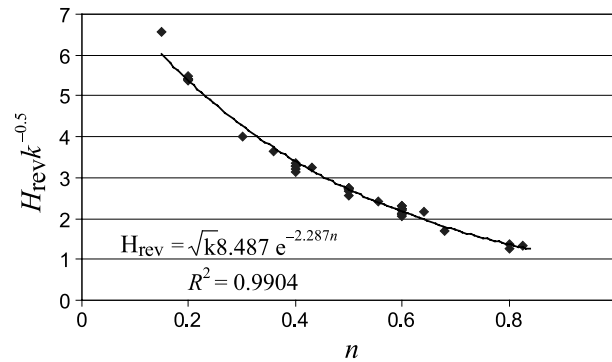


Figure 4. The fitted $f(n)$ function in the relationship between H_{rev} and the porous medium properties n and k (Eq. (11)).

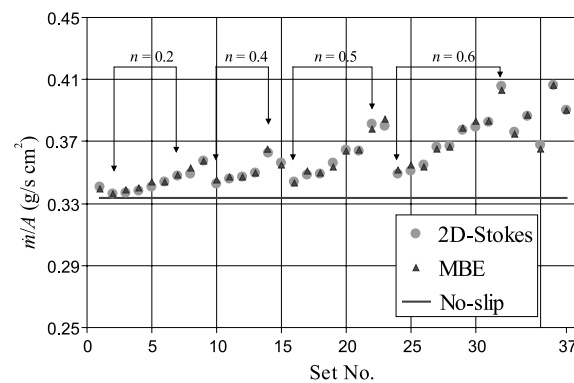


Figure 5. The mass flow rate above the porous surface in all the sets for $h = 10$ mm, obtained by integrating the 1D MBE and the 2D Stokes solutions. The continuous horizontal line represents the flow rate calculated for a laminar Poiseuille flow above an impermeable surface.

non-slip condition is applied at the top boundary (bounded flow). It was found (not shown here) that a good agreement exists between the micro-scale Stokes solution and the MBE prediction.

In many cases, an evaluation of flow rates is required. Figure 5 shows the mass flow rate above the porous media given $h = 10$ mm. The 1D MBE solution and the 2D Stokes solution were integrated and the resulting flow rates were compared. As expected, the flow rate increases with permeability (e.g. sets #2–#7 where $n = 0.2$ and k increases from 1.67×10^{-4} cm² (#2) to 2.667×10^{-3} cm² (#7)). Increasing the porosity leads to a moderate increase in flow rate (for example, sets #4, #12, #26, and #35). The continuous horizontal line in Figure 5 represents the flow rate calculated for a laminar Poiseuille flow above an impermeable surface. The flow rate above the porous interface is always higher than that above an impermeable surface. The influence of the porous interface on the flow rate increases as h decreases. Kim and Russell (1985) and Durlafsky and Brady (1987) claimed that the applicability of Brinkman equation is limited to porosities above 0.8 or even higher.

Figure 5 shows that the flow rate predicted by the modified Brinkman equation is accurate within a wide range of porosities (0.15–0.825).

The applicability of the Beavers and Joseph (1967) slip condition can now be examined. First, we note that the theoretical derivation of Beavers and Joseph (1967) slip condition was based on a one-dimensional Stokes solution, which predicts a linear shear profile. A good agreement with the Beavers and Joseph approach is not expected since the shear profile generated by the MBE is not linear. Such a non-linear shear profile was found by Sahraoui and Kaviany (1992) when they solved the micro-scale velocity field above an array of cylinders.

Beavers and Joseph (1967) developed their semi-empirical slip condition by measuring the flow rates above the porous interface and applying the laminar solution for a non-slip condition at the top. Since the top boundary condition of our unbounded flows is zero shear, the slip coefficient, α_{BJ} , is calculated using a modified expression. Given a slip velocity, $\langle u \rangle|_{z=0+}$, the mass flow rate in the non-porous region above a permeable interface ($k > 0$) is,

$$\dot{m}_{k>0} = \left(h \langle u \rangle|_{z=0+} - \frac{h^3}{3\mu} \frac{\partial \langle P \rangle}{\partial x} \right) \rho \tag{13}$$

We introduce the interface velocity gradient, $\partial \langle u \rangle / \partial z = -(h/\mu) \partial \langle P \rangle / \partial x$, into the Beavers and Joseph slip condition (Eq. (1)), replace $\langle u \rangle_d$ with $-(k/\mu) \partial \langle P \rangle / \partial x$ and solve it for the slip velocity,

$$\langle u \rangle|_{z=0+} = -\frac{\sqrt{k}}{\mu} \frac{\partial \langle P \rangle}{\partial x} \left[\sqrt{k} + \frac{h}{\alpha_{BJ}} \right] \tag{14}$$

Substituting Equation (14) into Equation (13), the slip coefficient α_{BJ} is recovered,

$$\alpha_{BJ} = h \left(\frac{\Phi h^2}{3\sqrt{k}} - \sqrt{k} \right)^{-1} \tag{15}$$

where Φ , the relative increase in mass flow rate above the porous media, is defined as

$$\Phi = \frac{\dot{m}_{k>0} - \dot{m}_{k=0}}{\dot{m}_{k=0}} \tag{16}$$

$\dot{m}_{k=0}$ being the mass flow rate above an impermeable surface ($-(h^3/3\mu) \partial \langle P \rangle / \partial x$). Equation (15) allows us to calculate the slip coefficient in an indirect way, without the need to calculate the shear rate at the interface.

The Taylor brush problem (Taylor, 1971), which is composed of repeated grooves of width s separated by walls of width t , was treated theoretically by Richardson (1971). Using an asymptotic solution, the following expression for α_{BJ} was obtained

$$\alpha_{BJ} \sim \frac{2\pi k^{0.5}}{t \ln t + (t + 2s) \ln(t + 2s) - 2(t + s) \ln(t + s)} \tag{17}$$

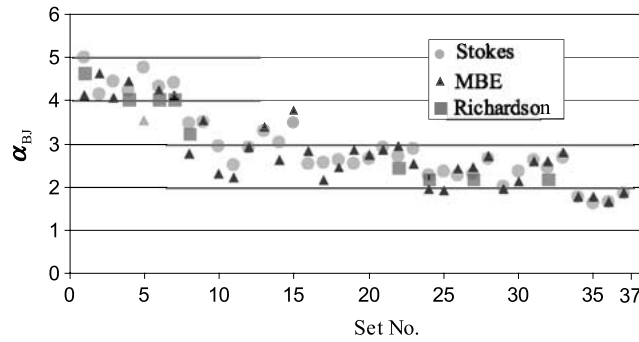


Figure 6. The Beavers and Joseph slip coefficient, α_{BJ} , calculated by Equation (15) for all 37 sets. Mass flow rate was produced by solving the 1D MBE and the 2D Stokes equations, for $h = 10$ mm. α_{BJ} was also calculated by Richardson (1971) expression (Eq. (17)) for sets #1, #4, #6, #7, #8, #22, #24, #27 and #32.

where the permeability is $k = s^3/12(t + s)$. The comparison with Richardson (1971) expression was therefore limited to sets with grooves arrangement similar to that analyzed by Taylor (1971) and Richardson (1971) (sets #1, #4, #6, #7, #8, #22, #24, #27 and #32). Figure 6 presents the Beavers and Joseph slip coefficient as calculated by the MBE, the micro-scale Stokes solutions and the Richardson expression (Eq. (17)). The MBE and Stokes solutions were obtained for $h = 10$ mm. Figure 6 shows that the overall agreement between the slip coefficients obtained by the MBE and those resulting from the Stokes equation and the Richardson expression is good, and seems to improve with porosity. However, the behavior of the slip coefficient with respect to variations in porosity and permeability is somehow jumpy. As in Richardson's work, the analysis of our more general case shows that as the porosity increases, the Beavers and Joseph slip coefficient decreases. This is opposite to the findings of Sahraoui and Kaviany (1992) showing that α_{BJ} increases with porosity. Indeed, the calculation in Sahraoui and Kaviany (1992) was made for a constant Reynolds number, while our results are presented for a constant pressure gradient. However, we think that this condition better represents a steady surface flow on a given slope.

5. Conclusions

It is shown that the interface macroscopic velocity of a shallow laminar flow above a porous surface can be accurately modeled by introducing a modification to the Brinkman equation (MBE). Based on the numerical solution of the 2D Stokes equation for 37 geometrical sets representing brush configurations, the MBE was proved to be successful when choosing the correct representative elementary volume and comparing the macroscopic solution with the average microscopic flow. This result also applies when a non-slip condition is applied at the top boundary (bounded flow). Regardless the water height, the size of the representative elementary volume,

H_{rev} , was found to be equal to the product of the square root of the permeability and an exponential function of the porous medium porosity. Hence, a complete macroscopic solution of the interface flow is obtained for any brush configuration, given the fundamental properties of the porous media, n and k , the fluid viscosity, the flow height and the flow driving force dP/dx . This general solution may be applied to any laminar flow problem that involves an interface between a porous media that consists of series of grooves and a relatively fast moving flow region. This solution provides, also, an accurate description of the flow rate. As expected, the flow rate above the porous interface is always higher than that above an impermeable surface, and increases with the porous media porosity and permeability. The influence of the porous interface on the flow rate increases as the water height decreases. The results of the study show that the flow rate predicted by the MBE is accurate within a wide range of porosities (0.15–0.825), in contradiction with the conclusions of Kim and Russell (1985) and Durlofsky and Brady (1987) claiming that the applicability of the Brinkman equation is limited to high porosities.

Acknowledgements

The authors would like to acknowledge the Grand Water Research Institute at the Technion and the Joseph & Edith Fisher Career Development Chair for their generous funding.

References

- Adler, P. M. and Mills, P. M.: 1979, Motion and rupture of a porous sphere in a linear flow field, *J. Rheol.* **23**, 25–37.
- Basu, A. J. and Khalili, A.: 1999, Computation of flow through a fluid–sediment interface in a benthic chamber, *Phys. Fluids* **11**(6), 1395–1405.
- Beavers, G. S. and Joseph, D. D.: 1967, Boundary conditions at a naturally permeable wall, *J. Fluid Mech.* **30**, 197–207.
- Beavers, G. S., Sparrow, E. M. and Magnuson, R. A.: 1970, Experiments on coupled parallel flows in a channel and a bounding porous medium, *J. Basic Eng.* **92D** 843–848.
- Beavers, G. S., Sparrow, E. M. and Masha, B. A.: 1974, Boundary condition at a porous surface which bounds a fluid flow, *AIChE J.* **20**, 596–597.
- Brinkman, H. C.: 1947, A calculation of the viscous force exerted by a flowing fluid on a dense swarm of particles, *Appl. Sci. Res.* **1**, 27–34.
- Durlofsky, L. and Brady, J. F.: 1987, Analysis of the Brinkman equation as a model for flow in porous media, *Phys. Fluids* **30**, 3329.
- Gray, W. G. and O'Neill, K.: 1976, On the general equations for flow in porous media and their reduction to Darcy's law, *Water Resour. Res.* **12**, 148–154.
- Happel, J. and Brenner, H.: 1973, *Low Reynolds Number Hydrodynamics*, Noordhoff, Groningen, The Netherlands.
- Howells, I. D.: 1974, Drag due to the motion of a Newtonian fluid through a sparse random array of small rigid fixed objects, *J. Fluid Mech.* **64**, 449–475.
- James, D. F. and Davis, A. M. J.: 2001, Flow at the interface of a model fibrous porous medium, *J. Fluid Mech.* **426**, 47–72.

- Jennings, A. A. and Pisipati, R.: 1999, The impact of Brinkman's extension of Darcy's law in the neighborhood of a circular preferential flow pathway, *Environ. Model. Software* **14**, 427–435.
- Kaviany, M.: 1995, *Principles of Heat Transfer in Porous Media*, Springer, New York.
- Kim, S. and Russell, W. B.: 1985, Modeling of porous media by renormalization of the Stokes equations, *J. Fluid Mech.* **154**, 269–286.
- Koplik, J., Levine, H. and Zee, A.: 1983, Viscosity renormalization in the Brinkman equation, *Phys. Fluids* **26**, 2864–2870.
- Larson, R. E. and Higdon, J. J. L.: 1986, Microscopic flow near the surface of two-dimensional porous media. I. Axial flow, *J. Fluid Mech.* **166**, 449–472.
- Lundgren, T. S.: 1972, Slow flow through stationary random beds and suspensions of spheres, *J. Fluid Mech.* **51**, 273–299.
- Martys, N., Bentz, D. P. and Garboczi, E. J.: 1994, Computer simulation study of the effective viscosity in Brinkman's equation, *Phys. Fluids* **6**(4), 1434–1439.
- Nield, D. A. and Bejan, A.: 1992, *Convection in Porous Media*, Springer, New York, pp. 11–19.
- Richardson, S.: 1971, A model for the boundary condition of a porous material. Part 2, *J. Fluid Mech.* **49**, 327–336.
- Saffman, P. G.: 1971, On the boundary condition at the surface of a porous medium, *Stud. Appl. Math.* **2**, 93–101.
- Sahraoui, M. and Kaviany, M.: 1992, Slip and no-slip velocity boundary-conditions at interface of porous, plain media, *Int. J. Heat Mass Transfer* **35**(4), 927–943.
- Shavit, U., Bar-Yosef, G., Rosenzweig, R. and Assouline, S.: 2002, Modified Brinkman equation for a free flow problem at the interface of porous surfaces: the Cantor–Taylor brush configuration case, *Water Resour. Res.* **38**, 1320–1334.
- Taylor, G. I.: 1971, A model for the boundary condition of a porous material. Part 1, *J. Fluid Mech.* **49**, 319–326.
- Vignes-Adler, M., Adler, P. M. and Gougat, P.: 1987, Transport processes along fractals. The Cantor–Taylor brush, *PhysicoChemical Hydrodyn.* **8**(4), 401–422.
- Whitaker, S.: 1999, *The Method of Volume Averaging*, Kluwer Academic Publishers, Dordrecht.
- Zhou, D. and Mendosa, C. C.: 1993, Flow through porous bed of turbulent stream, *J. Eng. Mech. ASCE* **119** 365–383.